Published in final edited form as:
Macromol Biosci. 2011 May 12; 11(5): 607–617. doi:10.1002/mabi.201000373.

Fabrication of DNA Polymer Brush Arrays by Destructive Micropatterning and Rolling-Circle Amplification

Kristopher D. Barbee[a], **Matt Chandrangsu**[a], and **Xiaohua Huang**[*]
Department of Bioengineering, University of California San Diego, 9500 Gilman Drive, La Jolla, CA 92093-0412, USA

Abstract

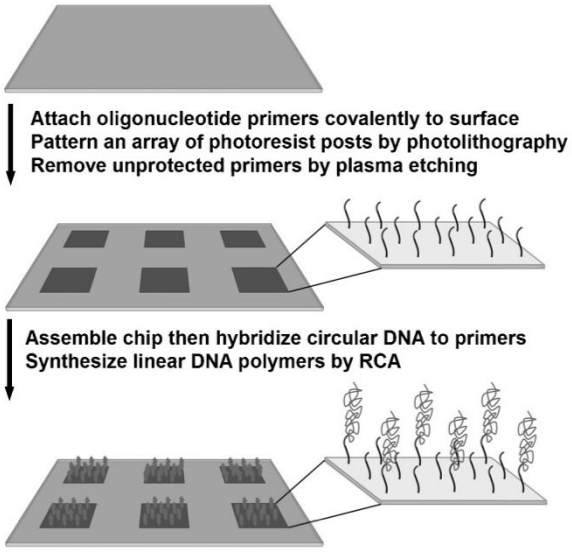

A method for fabricating DNA polymer brush arrays using photolithography and plasma etching followed by solid-phase enzymatic DNA amplification is reported. After attaching oligonucleotide primers to the surface of a glass coverslip, a thin layer of photoresist is spin-coated on the glass and patterned via photolithography to generate an array of posts in the resist. An oxygen-based plasma is then used to destroy the exposed oligonucleotide primers. The glass coverslip with the primer array is assembled into a microfluidic chip and DNA polymer brushes are synthesized on the oligonucleotide array by rolling-circle DNA amplification. We have demonstrated that the linear polymers can be rapidly synthesized in situ with a high degree of control over their density and length.

Keywords

DNA polymer brush arrays; functional coating; microfluidics; photolithography; solid-phase rolling circle amplification

[*]Fax: +1 858 534 5722; x2huang@ucsd.edu .
[a]K. D. B. and M. C. contributed equally to this work.

Introduction

High-density arrays of biomolecules can be fabricated by bottom-up approaches using cyclic synthesis and photolithography.[1] or robotic ink-jet printing.[2] They can also be fabricated by top-down approaches using robotic deposition with quill-pen[3] and dip-pen lithography,[4] microcontact printing,[5] or by assembling biomolecule-conjugated microbeads into arrays of wells.[6-9] These array technologies have enabled a myriad of high-throughput biological and chemical analyses on an unprecedented scale for genomic[10-12] and proteomic applications.[13] The biomolecules in these arrays, however, are presented either on a planar, two-dimensional (2D) surface or on the curved surface of a microbead. In contrast, arrays fabricated on substrates coated with porous polymer films or polymer brushes have been shown to provide higher loading capacities for the biomolecules and greater assay sensitivities.[14-19] Polymer brushes may provide a more optimal three-dimensional (3D) environment for assays and reactions such as DNA hybridization and PCR amplification. They can also be utilized to control molecular interactions, and to reduce non-specific adsorption on surfaces.[20,21]

Polymer brushes can be fabricated by either “grafting to” or “grafting from” techniques. The grafting to process is a top-down approach in which polymers pre-synthesized in solution are adsorbed or covalently attached to a suitable substrate. In contrast, the grafting from method is a bottom-up approach in which polymers are synthesized in situ by controlled radical polymerization techniques.[22,23] Even though long linear polymers of various lengths can be synthesized in solution, creating dense and thick polymer brushes on a surface with the top-down approach can be very difficult. This is due to the limited packing density that can be achieved with long linear polymers, which assume random-coiled conformations with an average radius much greater than the diameter of the backbone of the polymers in a good solvent.[24-26] On the other hand, denser polymer brushes can be produced by the bottom-up approach but the characterization of these polymers can be difficult and typically requires complex tools and techniques.[24]

As an alternative to the traditional controlled radical polymerization techniques, we have developed an enzymatic approach for the in situ synthesis of thick, dense polymer brushes. We utilize DNA polymerases to synthesize linear DNA molecules by solid-phase rolling-circle amplification (RCA).[27-31] First, the oligonucleotide primers are covalently attached to the surface. Second, circular DNA templates are hybridized to the primers. Third, DNA polymerases are used to synthesize long linear DNA polymers by replicating the circular DNA molecules. Unlike passive radical polymerization, enzymatic polymerization is actively powered by the DNA polymerases, which catalyze the reaction and convert the chemical energy of phosphodiester bond hydrolysis into locomotion. We have demonstrated that the density and length of these single-stranded DNA (ssDNA) polymer brushes can be controlled by simply varying the number of circular template molecules available for hybridization to the surface-bound primers and the duration of the amplification process, respectively. We have also shown that these DNA polymers can be easily characterized by fluorescence microscopy and basic molecular biology techniques. Various chemical moieties may be added to these polymers by the incorporation of modified nucleotides during synthesis[32] or the post-synthesis hybridization and cross-linking of oligonucleotides with desired functional groups.[33] These functionalized DNA polymer brushes may then serve as a means to overcome the limitations of 2D surface-bound biomolecular assays and reactions.

We also report a method for fabricating high-density arrays of these DNA polymer brushes to facilitate high-throughput, multiplexed assays and reactions via spatial separation and confinement. As shown in Figure 1, the DNA polymers are synthesized by RCA on DNA

oligonucleotide arrays that have been fabricated via a destructive micropatterning technique. The microfabrication process utilizes photolithography to create a dense array of posts in photoresist on a glass substrate derivatized with DNA oligonucleotides and poly(ethylene glycol) (PEG) molecules. A subsequent exposure to oxygen plasma is then performed to destroy the biomolecules in the regions that are not protected by the photoresist.[34] The posts are then removed with organic solvents to expose the remaining DNA and PEG molecules. These oligonucleotides later serve as primers for the synthesis of long, ssDNA polymers via RCA on circularized DNA molecules. The reaction is performed within a microfluidic chip that is placed in a device with precision heating and cooling capabilities (Figure 2). Upon completion of the reaction and subsequent hybridization of fluorescently labeled DNA probes, the polymers are observed by epifluorescence microscopy. Enzymatic digestion of the RCA products can also be performed to estimate the length of the polymers, the total amount of DNA synthesized on the array and the polymer density. Our ability to control the length and density of these RCA products will enable us to optimize biomolecule loading and the efficiency of enzymatic reactions performed on these polymers by minimizing steric hindrance.[35,36]

Experimental Part

Processing and Activation of Substrates

Custom glass coverslips with dimensions of 50 × 75 × 0.170 mm^3 (Erie Scientific Co.) were used as the substrates and derivatized with carboxylate groups on the surface. The coverslips were cleaned by sonication for 1 h in a 2% solution of Micro-90 (Cole-Parmer Instrument Co.) in batch mode using a custom-built PTFE rack, rinsed five times with deionized water (dH_2O, 18 MΩ · cm, Millipore Milli-Q) and then cleaned in a 1:1:5 solution of NH_4OH/H_2O_2/H_2O at 85 °C for 1 h (caution: This mixture is extremely dangerous and should be handled with care). The coverslips were further cleaned in a 3:1 solution of H_2SO_4/H_2O_2 at 85 °C for 1 h and then rinsed extensively with dH_2O (caution: This mixture is extremely dangerous and should be handled with care). The substrates were dipped briefly in ethanol and then soaked in a 2% solution of 3-aminopropyltriethoxysilane in 95:5 of ethanol/dH_2O for 5 min to functionalize the surface with primary amine groups. After rinsing three times in acetone, the coverslips were baked at 110 °C for 10 min. Terminal carboxylic acid groups were then generated by soaking the coverslips for 2 h in a solution of 0.250 M succinic anhydride and 0.250 M dry triethylamine in dry dimethylformamide (DMF). After rinsing three times with acetone, the coverslips were dried by blowing with filtered, compressed air and then stored under vacuum until further use.

Conjugation of Oligonucleotide Primers to Glass Coverslips

The oligonucleotides used in this study were synthesized and purified by Integrated DNA Technologies. All primers and templates were designed to minimize intra-molecular self-hybridization and inter-molecular cross-hybridization. The amine-labeled primers for covalent attachment to the surface for solid-phase RCA have one of the following two sequences: 5′-NH_2-$(CH_2)_6$-TTT TTT TTT TTT TTT TTT TTT TTT TTT TTT TTT TTT TTT TTT TTA CGT CGT CCG TGC TAG AAG GAA ACA CGC AAT GAT CAC AGC TGA GGA TAG GAC ATG CGA-3′ or 5′-NH_2-$(CH_2)_6$-TTT TTT TTT TTT TTT TTT TTT TTT TTT TTT TTT TTT TTT TTT TTT TTT TTT TTT TTT TTT TTT TTA TGA TCA CAG CTG AGG ATA GGA CAT GCG AAC GTC GTC CGT GCT AGA AGG AAA CAC GCA ACG TCG TCC GTG CTA GAA GGA AAC ACG CA-3′. The first 50 deoxythymidine residues serve as a spacer between the surface and the priming region. The next 29 bases are present to allow the RCA product to be cut from the surface of the chip using an endonuclease such as BanI or PvuII. The last 29 bases serve as the priming region for the circularized templates described below. The oligonucleotides were covalently attached to the glass or silicon

dioxide surface via amide bonds by reacting the primary amine group on the oligonucleotide with the carboxylic acid groups on the substrate. A 10^{-6} M solution of the 5′-amine-labeled oligonucleotides with 0.180 M 1-ethyl-3-(3-dimethylaminopropyl)carbodiimide (EDC) in 2-(*N*-morpholino)-ethanesulfonic acid (MES)/borate buffer (0.050 M MES, 0.025 M borate, pH = 4.8) was spotted onto the carboxylated glass coverslip, covered with a second carboxylated coverslip, and incubated in a humid chamber for 90 min at room temperature. A 22 × 22 × 0.15 mm^3 coverslip was placed in between the two larger coverslips to maintain adequate separation during the incubation and assist in their separation. Following the derivatization step, the coverslips were rinsed three times with dH_2O and then blown dry with filtered, compressed air.

Conjugation of PEG Molecules to Glass Coverslips

PEG molecules were conjugated to the residual carboxyl groups immediately following the DNA conjugation process. A solution containing 10^{-2} M of a methyl-$(OCH_2CH_2)_{24}$-amine compound (Cat. # 26116, Thermo Fisher Scientific) and 0.100 M EDC in MES-Borate buffer was spotted onto a DNA-conjugated coverslip and covered with a second DNA-conjugated coverslip as described above. Following a 30–90 min incubation at room temperature, the coverslips were rinsed with dH_2O then stored in a 5X-SSC-T solution (5X-SSC-T: 5X SSC solution with 0.1% Triton X-100, where a 1X SSC solution contains 1.5 × 10^{-2} M sodium citrate and 0.150 M NaCl, pH = 7.0) until further use.

Fabrication of Primer Arrays by Photolithography and Destructive Patterning

Immediately prior to patterning, the coverslips with covalently conjugated oligonucleotide primers were rinsed three times with dH_2O and blown dry with dry nitrogen. The coverslips were then coated with a thin layer of positive photoresist (Shipley Microposit S1813, Rohm & Haas Electronic Materials) by spinning at 6 000 rpm for 30 s. The coverslips were baked at 85 °C on a hotplate for 2 min and then patterned via photolithography on a MA/BA6 contact aligner (SUSS MicroTec). A photomask containing chrome contacts on a clear background was used to create arrays of posts in the resist. The resist was developed for 60–90 s in MF-321 (Rohm & Haas Electronic Materials), rinsed with dH_2O and then blown dry with dry nitrogen. DNA primers not protected by the photoresist were completely destroyed by exposing the patterned coverslips to oxygen-based plasma for 3 min at 100 W and 300 mTorr in a Technics PE-IIB plasma system. The remaining photoresist was removed by soaking the coverslips in Shipley Microposit Remover 1165 (Rohm & Haas Electronic Materials) at 70 °C for 15 min. The coverslips were then rinsed three times in acetone, three times with dH_2O, and then stored in a 5X-SSC-T solution until further use. This fabrication process is illustrated in Figure 1.

Assembly of Microfluidic Chips

Holes were drilled in 50 × 75 × 1 mm^3 glass slides (Product # 2947–75X50, Corning) using a 1-mm diamond-coated drill bit (Cat. # MD16, C.R. Laurence Co) and a high-speed rotary tool (Mod. # 38481, Proxxon) mounted to a CNC milling machine (Mod. # PCNC 1100, Tormach). The drilling process was performed under water or a dilute coolant solution (Formula 77, Kool Mist) The slides were cleaned by the same process used to clean the coverslips and then attached to the patterned coverslips using a ≈110 μm-thick, double-sided silicone adhesive tape (Scapa 702, Scapa Group). The coverslips were rinsed three times with dH_2O and blown dry with dry, compressed air immediately prior to the chip assembly process. The cutouts that form the fluidic channels in the chip were designed using AutoCAD (AutoDesk) and Illustrator CS3 (Adobe Systems) then cut out of the tape using a cutting plotter (Mod. # GX-24 CAMM-1, Roland). Each chip contained six 30 mm long and 2 mm wide channels.

Fabrication and Operation of the Microfluidic Device

A device was designed and constructed to enable precise, automated heating and cooling of the chip, and automated delivery of reagents. An exploded view and photograph of this device is shown in Figure 2. The heat sink and cold plate were machined out of 6061 aluminum alloy. The coverslip of the assembled chip sits on top of the heating and cooling plate while the fluidic connections are made to the chip via holes in the slide through ports in a thick polycarbonate block. Silicone rubber O-rings (Cat. # 006570, McMaster-Carr Co.) are used at the interface between the glass slide and top block to create leak-free seals. The polycarbonate block is compressed against the chip with springs. Two pairs of thermoelectric modules (Cat. # VT-199-1.4-1.5, TE Technology) operated in a cascade configuration are used for heating and cooling. The power to the modules is provided by a power supply (Cat. # PS-24-20, TE Technology) via a controller board (Cat. # TC-24-25R, TE Technology). A thermistor (Cat. # MP-2444, TE Technology) is embedded in a shallow groove in the aluminum plate to provide temperature sensing. The temperature of the device is controlled by the proportional-integral-derivative method via a PC using LabVIEW v8.0 (National Instruments). The heat sink is kept at 20 °C using a refrigerated circulator (RTE-111, Neslab Instruments). A multi-channel syringe pump (Cavro XL 3000, Tecan Group) connected to the device via flangeless fittings (Cat. # P-252/P-259, Upchurch Scientific) is used to deliver reagents and wash solutions. Check valves (Cat. # EW-01355-14, Cole Parmer Instrument Co.) are used to prevent back-flow when removing the polycarbonate block. The pump is controlled via Pump:Link software (Tecan Group).

Preparation of Circular DNA Molecules

Two different circular DNA molecules, Circle1 and Circle2, were prepared from 78-base long linear oligonucleotides with the following sequences: 5′-phosphate-CTC AGC TGT GAT CAT CAG AAC TCA CCT GTT AGA CGC CAC CAG CTC CAA CTG TGA AGA TCG CTT ATC GCA TGT CCT ATC-3′ (LC1) or 5′-phosphate-CAC GGA CGA CGT ATA TGA TGG TAC CGC AGC CAG CAT CAC CAG ACT GAG TAT CTC CTA TCA CTG CGT GTT TCC TTC TAG CAC GGA CGA CGT-3′ (LC2). A guide oligonucleotide (5′-ATG ATC ACA GCT GAG GAT AGG ACA TGC GA-3′ for Circle1 or 5′-ACG TCG TCC GTG CTA GAA GGA AAC ACG AC-3′ for Circle2), with sequence complementary to both ends of the 78-base linear oligonucleotide was used to bring the 3′ end and 5′ phosphorylated end to a juxtaposed position for ligation. To purify the circularized DNA molecules, the guide oligos and unligated linear oligos were removed by exonuclease digestion. Specifically, the circular DNA molecules were created as follows: 10^{-6} M of the linear oligo was hybridized to 1.1×10^{-6} M of the guide sequence in a ligase buffer [0.020 M of TrisCl, 0.025 M KCl, 10^{-2} M $MgCl_2$, 10^{-3} M ATP, 5×10^{-3} M DTT, 100 $\mu g \cdot mL^{-1}$ BSA (Cat. # 10711454001, Roche), pH = 7.5] by heating at 75 °C for 5 min and cooling slowly down to 22 °C. BSA (Cat. # 10711454001, Roche) and T4 DNA Ligase (Cat. # 799099, Roche) were added to the solution to a final concentration of 100 $\mu g \cdot mL^{-1}$ and 0.25 $U \cdot \mu L^{-1}$, respectively. The ligation was carried out at 37 °C for 2 h and then the ligase was inactivated by heating at 80 °C for 10 min. The pH of the solution was then adjusted to 8.5 by adding an appropriate amount of a 1 M glycine solution (pH = 9.5). Exonuclease I and T7 Gene 6 Exonuclease (Cat. #s E70073X and E70025Z, United States Biochemicals) were then added to give a concentration of 1 $U \cdot \mu L^{-1}$ each and the digestion was carried out at 37 °C for 2 h. The enzymes were deactivated by heating at 80 °C for 10 min. The circularized DNA was extracted with phenol/chloroform and purified via ethanol precipitation. The DNA was dissolved in 10^{-2} M of TrisCl, pH = 7.5, analyzed, and quantified by polyacrylamide gel electrophoresis.

Synthesis of Linear DNA Polymers by RCA

Primer-conjugated substrates were re-hydrated by washing the channels with a 2X SSC solution with 1% SDS and heating at 90 °C for 15 min. The chip was then cooled to room temperature and the channels were washed for 2 min with a 2X-SSC-T solution (2X-SSC-T: 2X SSC solution with 0.1% Triton X-100). A solution containing 20 nM of Circle1 or Circle2 in a 2X SSC solution was then introduced and the chip was heated to 75 °C for 2 min and cooled to 55 °C at 2 °C · min^{-1}. The temperature was held at 55 °C for 15 min then cooled to 25 °C at a rate of 2 °C · min^{-1}. The channels were washed for 2 min in a polymerase buffer [0.020 M Tris-HCl, 10^{-2} M $(NH_4)_2SO_4$, 10^{-2} M KCl, 2×10^{-3} M $MgSO_4$, 0.1% Triton X-100, pH = 8.8 at 25 °C]. Bst DNA polymerase large fragment (Cat. # M0275L, New England Biolabs) was introduced at a concentration of 1 U · μL^{-1} in the polymerase buffer. The chip was then heated to 50 °C for 15 min to allow the polymerases to bind to the primed circular DNA molecules. The chip was cooled to 4 °C and a reaction mix containing 1 U · μL^{-1} Bst DNA polymerase, 100 μg · mL^{-1} BSA (Cat. # B9001S, New England Biolabs), 10^{-3} M each of dATP, dCTP, dGTP, and dTTP (Cat. #s 27-2050-02, 27-2060-02, 27-2070-02, and 27-2080-02, Amersham Biosciences), 4×10^{-6} M *Escherichia coli* single-stranded DNA binding protein (SSB, Cat. # 70032Z, United States Biochemicals) in a Bst buffer [0.020 M Tris-HCl, 10^{-3} M $(NH_4)_2SO_4$, 0.050 M KCl, 4×10^{-3} M $MgSO_4$, 0.1% Triton X-100, pH = 8.8 at 25 °C] was loaded. The chip was heated to 50 °C for the specified duration. The reactions were terminated by washing the channels with a wash buffer (2X SSC solution with 10^{-2} M EDTA and 0.1% Triton X-100). This process is illustrated in the last two steps in Figure 1.

Characterization by Fluorescence Imaging

Fluorescently labeled oligonucleotides were used for qualitative detection of the presence of the covalently-bound DNA primers and the RCA products. A Cy5-labeled oligonucleotide, 5′-Cy5- TCG CAT GTC CTA TCC TCA GCT GTG ATC AT-3′, was used to detect the surface-bound primers and a Cy3-labeled oligonucleotide, 5′-Cy3- TCA GAA CTC ACC TGT TAG AC-3′, was used to detect the RCA product from Circle1. The probes were introduced into the channels at a concentration of 10^{-6} M in a 2X SSC solution. The chip was heated to 75 °C for 2 min, and then cooled to 25 °C at a rate of 5 °C · min^{-1}. The channels were washed with a 2X-SSC-T solution and imaged using an epifluorescence microscope (Axio Observer.Z1, Carl Zeiss) with a 40× NA = 1.3 oil objective and a mercury arc lamp (X-Cite 120, EXFO Photonic Solutions) or a fast wavelength-switching light source with a 300W xenon arc lamp (Lambda DG-5, Sutter Instrument Co.). Scanning was performed using a BioPrecision 2 XY microscope stage and a MAC 5000 controller system (Ludl Electronics Products) and images were acquired with an EMCCD camera (iXon+885, Andor Technology). Auto-focusing was performed with a definite focus system (Carl Zeiss). Custom software was used for all hardware control and image acquisitions. Image analysis was performed with Image J.[37]

Characterization by Gel Electrophoresis

To quantify the amount of DNA polymer synthesized in a given channel, the RCA product generated from Circle2 on a non-patterned surface was digested in situ using a restriction enzyme which cuts only once in each repeat unit of the RCA product. First, a complimentary oligonucleotide, 5′-CGA CGT ATA TGA TGG TAC CGC AGC CAG CAT CAC CAG A-3′, was introduced at a concentration of 5.0×10^{-6} M in a 2X SSC solution and hybridized to the RCA product using the protocol described above. The channels were washed briefly with a reaction buffer (0.050 M potassium acetate, 0.020 M Tris acetate, 0.01 M magnesium acetate) and an enzyme solution containing 1 U · μL^{-1} BanI (Cat. # R0118L, New England Biolabs) in 0.050 M potassium acetate, 0.020 M Tris acetate, 0.010 M magnesium acetate, 100 μg · mL^{-1} BSA, and 10^{-3} M dithiothreitol, pH = 7.9 was introduced into the chamber and the

chip was incubated at 37 °C for ≈12 h. The digestion solution was collected from the chamber and analyzed using polyacrylamide gel electrophoresis. Solutions containing known amounts of the LC1 or LC2 oligonucleotides were also loaded onto the same gel for quantification purposes. The gel was stained with SYBR Gold (Cat. # S11494, Invitrogen) and imaged on a Gel Doc imaging system and analyzed using Discovery One software (Bio-Rad Laboratories). An ultralow-range gene ruler (Cat. # SM1211, Fermentas Life Sciences) was used as a molecular-weight marker.

To approximate the average polymer length and rate of DNA synthesis, the individual RCA products were cut and released from the surface of a non-patterned substrate using a restriction enzyme that cuts only at the base of each polymer. Following polymer synthesis, the channels were first washed with the reaction buffer. A mixture consisting of 0.2 $U \cdot \mu L^{-1}$ terminal transferase (TdT, Cat. # M0315L, New England Biolabs), 5×10^{-4} M dATP, 5×10^{-6} M ddATP (Cat. # 1008382, Roche) and 2.5×10^{-4} M $CoCl_2$ in the reaction buffer was then loaded and allowed to incubate at 37 °C for 30 min to add a poly-A tail onto the 3′ end of each DNA molecule. The enzyme was inactivated by heating the chip at 70 °C for 10 min. A poly-T oligonucleotide primer, 5′-TTT TTT TTT TTT TTT TTT TTT TTT T-3′ (PT25), at a concentration of 10^{-6} M in a 2X SSC solution was then hybridized to the polyA tails using the procedure described above. A reaction mix containing 0.1 $U \cdot \mu L^{-1}$ Phusion High-Fidelity DNA polymerase (Cat. # F530L, New England Biolabs), 10^{-3} M each of dATP, dCTP, dGTP, and dTTP, 4×10^{-7} M PT25 and 1X HF buffer (Cat. #F-518L, New England Biolabs) was loaded into the channels and the chip was heated at 67 °C for 15 min to convert all single-stranded DNA to a double-stranded form. The synthesis reaction was terminated by washing with the wash buffer and then the reaction buffer. A solution containing 2 $U \cdot \mu L^{-1}$ of PvuII (Cat. # R0151M, New England Biolabs) in a digestion buffer (0.050 M potassium acetate, 0.020 M Tris acetate, 0.010 M magnesium acetate, and 0.010 M dithiothreitol, pH = 7.9) was then loaded into the channels and the chip was incubated at 37 °C for ≈12 h. The solution was then collected from each channel and analyzed using agarose gel electrophoresis. The gel was stained, imaged, and analyzed as described above. The length of the RCA products was estimated from the gel using a 1 kb DNA Ladder (Cat. # N0468S, New England Biolabs) and a 1 kb Plus Ladder (Cat. # 10787-026, Invitrogen).

Characterization by Atomic Force Microscopy (AFM)

A scanning probe microscope (MultiMode, Veeco Instruments) with a Nanoscope IV controller was used in tapping mode to detect the overall height of the DNA polymer brush layers. The substrate with the patterned brush layer was scanned using an AFM probe tip (NP-10, Veeco Probes) with a nominal tip radius of 20 nm over a 12×12 μm^2 area at a rate of 1.34 Hz while submerged in a 2X SSC solution with 10^{-2} M EDTA and 0.1% Triton X-100.

Results and Discussion

Methods and Devices

We have developed a method for fabricating high-density arrays of oligonucleotides and DNA polymer brushes using a destructive micropatterning technique and solid-phase RCA. The micropatterning technique utilizes photolithography to generate an array of posts in photoresist on a DNA-conjugated substrate. Oxygen-based plasma is then used to destroy the oligonucleotides not protected by the photoresist. Once the resist is removed, the remaining oligonucleotides are used to synthesize linear DNA polymers using solid-phase RCA on circular DNA templates (Figure 1). Polymer synthesis is performed within microfluidic channels to minimize reagent use. A device with integrated temperature control and fluidics is employed to enable automated heating, cooling, and liquid handling (Figure

2). Fluorescently labeled complimentary oligonucleotides can be hybridized to the polymers to facilitate qualitative analysis by epifluorescence imaging (Figure 3). We also demonstrate the ability to control the polymer brush density and thickness by varying the amount of circular template loaded onto the substrate and RCA reaction time, respectively. Standard molecular biology techniques, which include enzymatic digestion and gel electrophoresis, were utilized for further characterization and quantification of these polymer brushes.

Using the oligonucleotide conjugation strategy described here, we found that it was necessary to cap any free carboxylic acid groups with aminated PEG molecules to enhance photoresist adhesion during the micropatterning process. Without this PEGylation step, a majority of the resist posts would detach from the substrate during development. Because the subsequent plasma etching step was employed to destroy oligonucleotides not protected by photoresist, the lost posts would result in polymer cluster drop-outs. Even with the inclusion of a PEGylation process, this type of defect was still occasionally observed (Figure 3). However, this defect rate was typically less than 0.1% and was likely caused by particle contamination on or within the substrate. The only other type of defect we observed was caused by limitations in the resolution and reproducibility of contact lithography. Consistent fabrication of high-density arrays is difficult because slight separation between the photomask and substrate will lead to significant interference defects. Poor contact can be caused by particle contamination or non-uniform substrate thickness. For a demonstration of principle, we used larger feature sizes in this study to minimize these defects due to the limitations of contact photolithography. However, much smaller feature sizes and higher densities can be achieved by using projection lithography.[9]

Control and Characterization of the Polymer Length and Density

The polymer density can be controlled by simply adjusting the number of circular templates that are available for hybridization to the surface-bound primers prior to the initiation of the RCA reaction. As shown in Figure 4, template concentrations below 2×10^{-9} M result in a polymer density at which some of the individual polymers can be resolved and counted in a fluorescent micrograph. At 2×10^{-10} M, the polymer density is low enough that nearly every polymer can be resolved and counted. To estimate the polymer density for the higher template concentrations, we have employed a strategy that involves the enzymatic digestion of the polymers on the chip and subsequent analysis by gel electrophoresis. The DNA polymers were either digested into 78-base fragments or cut just once near the attachment point. Oligonucleotides complementary to a specific sequence in each repeat of the RCA products was hybridized to the ssDNA polymers. The sequence contains a recognition site for a restriction enzyme, BanI, which is known to retain its activity even after long incubations. After digesting the polymers with BanI, the solution was reclaimed from the chip and analyzed on a 20% polyacrylamide gel. The result was a major band corresponding to the 78-base repeating unit. Using known amounts of LC1 or LC2 as standards, we were able to quantify the total number of copies of the 78-base circle that were synthesized on the chip during the RCA reaction (Figure 5).

Enzymatically cutting the polymers near the attachment point allowed for the removal and analysis of full-length polymer strands. First, a poly-A tail with an average length of 100 bases was added by a terminal transferase enzyme to the 3′ end of each strand using 100:1 molar ratio of dATP and ddATP. A short poly-T oligonucleotide was then hybridized to the poly-A tail and a DNA polymerase was used to convert the polymers into a double-stranded form. After the digestion with PvuII, the solution was reclaimed from the chip and analyzed on a 0.5% agarose gel with known DNA standards to determine the average length of the polymers (Figure 6).

The surface density of the DNA polymer brushes was estimated using the enzymatic digestion and gel electrophoresis data. First, the total number of 78-base tandem repeats synthesized within a given channel was obtained from the BanI digest data shown in Figure 5. Next, the average polymer length was estimated from the PvuII digestion data shown in Figure 6. These values were then used to estimate the polymer surface density, *d*, using the following relationship: $d = bc / LA$, where *b* is the number of bases per repeating unit, *c* is the number of repeating units per flow cell, *L* is the average number of bases in the full length polymer, and *A* is the total area of the flow cell occupied by the polymers. For an RCA reaction that began with the hybridization of a circular template at a concentration of 2×10^{-8} M, the average polymer density on a non-patterned surface was 153 molecules $\cdot \mu m^{-2}$. As shown in Figure 4, this density can be modified by adjusting the concentration of the circular template that is hybridized onto the surface-bound oligonucleotide primers. However, an extremely high polymer density may inhibit analysis by enzymatic digestion due to steric constraints.[35,36] Fortunately, this problem may be overcome through the use of various chemical cleavage methods.[38]

The limitations of these characterization methods include errors introduced by large polymer length distributions and the detection and sizing limits of gel electrophoresis. The polymer length distribution is minimized by pre-loading the primer-circle constructs with the DNA polymerase to synchronize the individual RCA reactions. Gel sizing limitations were dealt with by using relatively short RCA reaction times to keep the polymer lengths within reason. These short reaction times also helped to prevent the RCA molecules from growing long enough to bridge the gap between adjacent pads on the array (Figure 3D). The lower detection limit of gel electrophoresis was avoided by using non-patterned surfaces and circular template concentrations of at least 2×10^{-8} M. These steps helped ensure an adequate amount of DNA was synthesized within a given channel. However, a more sensitive gel electrophoresis system may enable the characterization of polymer brushes with even lower densities.

The features and thickness of the brush layers were also characterized by AFM in aqueous solution.[39] Figure 7 shows an AFM image of a region of a brush polymer array and the height profile of one feature on the array. There is a very clear contrast between the regions treated and not treated by the plasma but the measured height of 12 nm is much smaller than expected. For a freely-jointed chain conformation, the Flory radius of a 9 kb ssDNA molecule is estimated to be about 60 nm [$R_F = aN^{0.5} = 6.3 \times (9000)^{0.5} = 62$ nm, where a is the unit length of ssDNA with a value of ≈0.63 nm[40]].[25,26] However, the density of RCA-amplified linear DNA polymers is relatively low in this case, which provides sufficient space to accommodate the molecules close to the surface when a force is applied by the AFM tip.[41] Even with higher density brush polymer layers, forces applied by an AFM tip can cause the measured height to appear much lower than what is expected due to the displacement of the polymers directly under the tip.[42,43] Although the use of an electrolyte solution during AFM imaging has been used to reduce this compression, it also causes the polymer to take a collapsed state, thus changing its effective height.[44] Further work will be required to investigate the conformations and packing of the linear DNA molecules on the surface, and to control the thickness of the brush layers.

Applications

There are many applications for polymer brushes in biotechnology and nanotechnology.[18,19,21,45] In one potential application, these DNA polymer brushes may serve as long, flexible supports for the attachment of various biomolecules. For instance, attaching multiple PCR primers along the length of these polymers may enable greater primer accessibility for more efficient DNA amplification than what can be achieved using traditional solid-phase PCR (SP-PCR). The inefficiencies of SP-PCR,[17] which requires a

large number of reaction cycles to achieve a relatively small number of template copies,[38,46] is attributed to poor hybridization efficiencies and steric constraints. However, the use of polymer-bound oligonucleotide primers may provide a more favorable environment for PCR, which is likely to result in the synthesis of more template copies in fewer cycles. In essence, the DNA polymers create a 3D, solution-like environment that may enable more efficient reactions than possible on 2D substrates.[17] In addition, the greater loading capacities afforded by the third dimension of the polymers may allow for the synthesis of many more template copies on a spot on an array[14] or on the surface of a microbead,[47] which may be advantageous to both microbead- and surface-based DNA sequencing platforms.[48-50] This third dimension may also enable further reductions in the spot size on DNA microarrays without compromising the dynamic range needed for gene expression analysis.[51]

Another potential advantage of the technology presented here is the isolation of the polymer clusters afforded by the array format. With each cluster of DNA polymers spatially separated from one another, the products of individual clonal DNA amplification reactions, or amplicons, would also remain separated from each other.[14,38] The ability to confine these reactions may prove beneficial to current DNA sequencing platforms by eliminating amplicon overlap and controlling amplicon size. These issues represent significant challenges in that DNA template concentrations must be carefully controlled to ensure an optimal amplicon density is obtained.[38,50] High amplicon densities typically result in excessive overlap whereas low densities result in poor throughput. Restricting the outward growth of the amplicon may even result in higher template densities if the amplification process continues to generate additional template copies that would effectively fill in the gaps within a given amplicon.[14,46] Furthermore, the use of an array format allows for higher imaging efficiencies to be obtained by reducing the number of unused pixels in each image and allowing each amplicon to be imaged with a minimal number of pixels.[7]

Conclusion

In summary, we have developed a method for fabricating high-density arrays of oligonucleotide primers using a destructive micropatterning technique. We have demonstrated that circular DNA molecules can be hybridized to these primers and amplified by RCA to generate an array of DNA polymer brushes. We have also shown that these DNA polymers brushes can be well characterized by fluorescence imaging, enzymatic digestion, and gel electrophoresis. These long, linear polymers may be useful for enhancing the sensitivity and dynamic range of biomolecular assays by enabling higher loading capacities and more efficient biomolecular binding. The 3D, solution-like environment created by these DNA polymer brushes may also enable more efficient enzymatic reactions such as solid-phase DNA amplification.

Acknowledgments

This work was supported by grants from the *National Human Genome Research Institute* (HG004804 and HG004130) and the *National Science Foundation* under a career award to X. H. (BES-0547193). A portion of this work was performed in the *Nano3 facility at CalIT*^{2} at UCSD. We thank *Larry Grissom* and *Ryan Anderson* for training and technical support at Nano3. We thank *Aric Joneja* for advice regarding enzymes, primers, and DNA amplification strategies. We also thank *Eric Roller* for programming the automated imaging system.

References

[1]. Fodor SP, Rava RP, Huang XC, Pease AC, Holmes CP, Adams CL. Nature. 1993; 364:555. [PubMed: 7687751]

[2]. Lausted CG, Warren CB, Hood LE, Lasky SR. Methods Enzymol. 2006; 410:168. [PubMed: 16938551]

[3]. Schena M, Shalon D, Davis RW, Brown PO. Science. 1995; 270:467. [PubMed: 7569999]

[4]. Piner RD, Zhu J, Xu F, Hong S, Mirkin CA. Science. 1999; 283:661. [PubMed: 9924019]

[5]. Lange SA, Benes V, Kern DP, Horber JKH, Bernard A. Anal. Chem. 2004; 76:1641. [PubMed: 15018562]

[6]. Ferguson JA, Steemers FJ, Walt DR. Anal. Chem. 2000; 72:5618. [PubMed: 11101240]

[7]. Barbee KD, Huang X. Anal. Chem. 2008; 80:2149. [PubMed: 18260655]

[8]. Blicharz TM, Siqueira WL, Helmerhorst EJ, Oppenheim FG, Wexler PJ, Little FF, Walt DR. Anal. Chem. 2009; 81:2106. [PubMed: 19192965]

[9]. Barbee KD, Hsiao AP, Heller MJ, Huang X. Lab Chip. 2009; 9:3268. [PubMed: 19865735]

[10]. Chee M, Yang R, Hubbell E, Berno A, Huang XC, Stern D, Winkler J, Lockhart DJ, Morris MS, Fodor SP. Science. 1996; 274:610. [PubMed: 8849452]

[11]. Schena M, Shalon D, Heller R, Chai A, Brown PO, Davis RW. Proc. Natl. Acad. Sci. USA. 1996; 93:10614. [PubMed: 8855227]

[12]. Gunderson KL, Steemers FJ, Lee G, Mendoza LG, Chee MS. Nat. Genet. 2005; 37:549. [PubMed: 15838508]

[13]. Zhu H, Bilgin M, Bangham R, Hall D, Casamayor A, Bertone P, Lan N, Jansen R, Bidlingmaier S, Houfek T, Mitchell T, Miller P, Dean RA, Gerstein M, Snyder M. Science. 2001; 293:2101. [PubMed: 11474067]

[14]. Mitra R, Church G. Nucleic Acids Res. 1999; 27:e34. [PubMed: 10572186]

[15]. Kusnezow W, Hoheisel JD. J. Mol. Recognit. 2003; 16:165. [PubMed: 12898667]

[16]. Miller JC, Zhou H, Kwekel J, Cavallo R, Burke J, Butler EB, Teh BS, Haab BB. Proteomics. 2003; 3:56. [PubMed: 12548634]

[17]. Pemov A, Modi H, Chandler DP, Bavykin S. Nucleic Acids Res. 2005; 33:e11. [PubMed: 15661850]

[18]. Ishihara K, Takai M. J. R. Soc. Interface. 2009; 6:S279. [PubMed: 19324688]

[19]. Jain P, Baker GL, Bruening ML. Annu. Rev. Anal. Chem. 2009; 2:387.

[20]. Hoy O, Zdyrko B, Lupitskyy R, Sheparovych R, Aulich D, Wang J, Bittrich E, Eichhorn K-J, Uhlmann P, Hinrichs K, Müller M, Stamm M, Minko S, Luzinov I. Adv. Funct. Mater. 2010; 20:2240.

[21]. Hucknall A, Kim D-H, Rangarajan S, Hill RT, Reichert WM, Chilkoti A. Adv. Mater. 2009; 21:1968.

[22]. Matyjaszewski K, Xia J. Chem. Rev. 2001; 101:2921. [PubMed: 11749397]

[23]. Zhao B, Brittain WJ. Prog. Polym. Sci. 2000; 25:677.

[24]. Tomlinson MR, Cousin F, Geoghegan M. Polymer. 2009; 50:4829.

[25]. Flory PJ, Fox TG Jr. J. Polym. Sci. 1950; 5:745.

[26]. Flory, PJ. Statistical Mechanics of Chain Molecules. Inter-science Publishers; New York: 1969.

[27]. Fire A, Xu SQ. Proc. Natl. Acad. Sci. USA. 1995; 92:4641. [PubMed: 7753856]

[28]. Liu D, Daubendiek SL, Zillman MA, Ryan K, Kool ET. J. Am. Chem. Soc. 1996; 118:1587. [PubMed: 20830216]

[29]. Lizardi PM, Huang X, Zhu Z, Bray-Ward P, Thomas DC, Ward DC. Nat. Genet. 1998; 19:225. [PubMed: 9662393]

[30]. Hatch A, Sano T, Misasi J, Smith CL. Genet. Anal. - Biomol. Eng. 1999; 15:35.

[31]. McCarthy EL, Bickerstaff LE, Cunha M. Pd. Millard PJ. Biosens. Bioelectron. 2007; 22:1236. [PubMed: 16797962]

[32]. Kuwahara M, Hososhima S-i. Takahata Y, Kitagata R, Shoji A, Hanawa K, Ozaki AN, Ozaki H, Sawai H. Nucleic Acids Symp. 2003; 3:37.

[33]. Pieles U, Englisch U. Nucleic Acids Res. 1989; 17:285. [PubMed: 2911468]

[34]. Flounders AW, Brandon DL, Bates AH. Biosens. Bioelectron. 1997; 12:447. [PubMed: 9253151]

[35]. Castronovo M, Radovic S, Grunwald C, Casalis L, Morgante M, Scoles G. Nano Lett. 2008; 8:4140. [PubMed: 19367999]

[36]. Bar M, Bar-Ziv RH. Nano Lett. 2009; 9:4462. [PubMed: 19835406]

[37]. Abramoff MD, Magelhaes PJ, Ram SJ. Biophotonics Intl. 2004; 11:36.

[38]. Fedurco M, Romieu A, Williams S, Lawrence I, Turcatti G. Nucleic Acids Res. 2006; 34:e22. [PubMed: 16473845]

[39]. Hansma HG, Pietrasanta LI, Auerbach ID, Sorenson C, Golan R, Holden PA. J. Biomater. Sci., Polym. Ed. 2000; 11:675. [PubMed: 11011766]

[40]. Murphy MC, Rasnik I, Cheng W, Lohman TM, Ha T. Biophys. J. 2004; 86:2530. [PubMed: 15041689]

[41]. Subramanian G, Williams DRM, Pincus PA. Macromolecules. 1996; 29:4045.

[42]. Murat M, Grest GS. Macromolecules. 1996; 29:8282.

[43]. Kelley TW, Schorr PA, Johnson KD, Tirrell M, Frisbie CD. Macromolecules. 1998; 31:4297.

[44]. Farhan T, Azzaroni O, Huck WTS. Soft Matter. 2005; 1:66.

[45]. Ayres N. Polym. Chem. 2010; 1:769.

[46]. Adessi C, Matton G, Ayala G, Turcatti G, Mermod J-J, Mayer P, Kawashima E. Nucleic Acids Res. 2000; 28:e87. [PubMed: 11024189]

[47]. Dressman D, Yan H, Traverso G, Kinzler KW, Vogelstein B. Proc. Natl. Acad. Sci. USA. 2003; 100:8817. [PubMed: 12857956]

[48]. Margulies M, Egholm M, Altman WE, Attiya S, Bader JS, Bemben LA, Berka J, Braverman MS, Chen YJ, Chen Z, Dewell SB, Du L, Fierro JM, Gomes XV, Godwin BC, He W, Helgesen S, Ho CH, Irzyk GP, Jando SC, Alenquer MLI, Jarvie TP, Jirage KB, Kim J-B, Knight JR, Lanza JR, Leamon JH, Lefkowitz SM, Lei M, Li J, Lohman KL, Lu H, Makhijani VB, McDade KE, McKenna MP, Myers EW, Nickerson E, Nobile JR, Plant R, Puc BP, Ronan MT, Roth GT, Sarkis GJ, Simons JF, Simpson JW, Srinivasan M, Tartaro KR, Tomasz A, Vogt KA, Volkmer GA, Wang SH, Wang Y, Weiner MP, Yu P, Begley RF, Rothberg JM. Nature. 2005; 437:376. [PubMed: 16056220]

[49]. Shendure J, Porreca GJ, Reppas NB, Lin X, McCutcheon JP, Rosenbaum AM, Wang MD, Zhang K, Mitra RD, Church GM. Science. 2005; 309:1728. [PubMed: 16081699]

[50]. Bentley DR, Balasubramanian S, Swerdlow HP, Smith GP, Milton J, Brown CG, Hall KP, Evers DJ, Barnes CL, Bignell HR, Boutell JM, Bryant J, Carter RJ, Keira Cheetham R, Cox AJ, Ellis DJ, Flatbush MR, Gormley NA, Humphray SJ, Irving LJ, Karbelashvili MS, Kirk SM, Li H, Liu X, Maisinger KS, Murray LJ, Obradovic B, Ost T, Parkinson ML, Pratt MR, Rasolonjatovo IMJ, Reed MT, Rigatti R, Rodighiero C, Ross MT, Sabot A, Sankar SV, Scally A, Schroth GP, Smith ME, Smith VP, Spiridou A, Torrance PE, Tzonev SS, Vermaas EH, Walter K, Wu X, Zhang L, Alam MD, Anastasi C, Aniebo IC, Bailey DMD, Bancarz IR, Banerjee S, Barbour SG, Baybayan PA, Benoit VA, Benson KF, Bevis C, Black PJ, Boodhun A, Brennan JS, Bridgham JA, Brown RC, Brown AA, Buermann DH, Bundu AA, Burrows JC, Carter NP, Castillo N, Chiara M, Catenazzi E, Chang S, Neil Cooley R, Crake NR, Dada OO, Diakoumakos KD, Dominguez-Fernandez B, Earnshaw DJ, Egbujor UC, Elmore DW, Etchin SS, Ewan MR, Fedurco M, Fraser LJ, Fuentes Fajardo KV, Scott Furey W, George D, Gietzen KJ, Goddard CP, Golda GS, Granieri PA, Green DE, Gustafson DL, Hansen NF, Harnish K, Haudenschild CD, Heyer NI, Hims MM, Ho JT, Horgan AM, Hoschler K, Hurwitz S, Ivanov DV, Johnson MQ, James T, Huw Jones TA, Dong Kang G, Kerelska TH, Kersey AD, Khrebtukova I, Kindwall AP, Kingsbury Z, Kokko-Gonzales PI, Kumar A, Laurent MA, Lawley CT, Lee SE, Lee X, Liao AK, Loch JA, Lok M, Luo S, Mammen RM, Martin JW, McCauley PG, McNitt P, Mehta P, Moon KW, Mullens JW, Newington T, Ning Z, Ling Ng B, Novo SM, O'Neill MJ, Osborne MA, Osnowski A, Ostadan O, Paraschos LL, Pickering L, Pike AC, Pike AC, Chris Pinkard D, Pliskin DP, Podhasky J, Quijano VJ, Raczy C, Rae VH, Rawlings SR, Chiva Rodriguez A, Roe PM, Rogers J, Rogert Bacigalupo MC, Romanov N, Romieu A, Roth RK, Rourke NJ, Ruediger ST, Rusman E, Sanches-Kuiper RM, Schenker MR, Seoane JM, Shaw RJ, Shiver MK, Short SW, Sizto NL, Sluis JP, Smith MA, Ernest Sohna Sohna J, Spence EJ, Stevens K, Sutton N, Szajkowski L, Tregidgo CL, Turcatti G, vandeVondele S, Verhovsky Y, Virk SM, Wakelin S, Walcott GC, Wang J, Worsley GJ, Yan J, Yau L, Zuerlein M, Rogers J, Mullikin JC, Hurles ME, McCooke

NJ, West JS, Oaks FL, Lundberg PL, Klenerman D, Durbin R, Smith AJ. Nature. 2008; 456:53. [PubMed: 18987734]

[51]. Dufva M. Biomol. Eng. 2005; 22:173. [PubMed: 16242381]

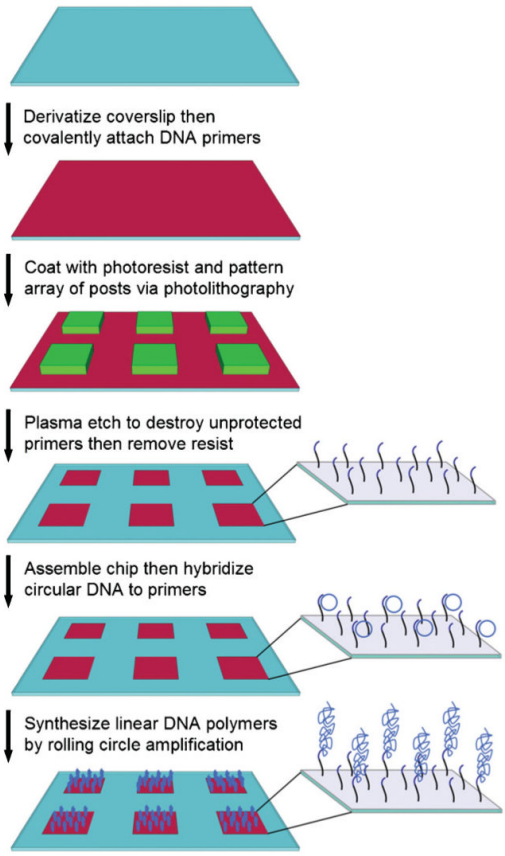

Figure 1.
Fabrication of DNA polymer brush arrays. Linear DNA polymer arrays are fabricated on glass coverslips using a destructive micropatterning technique and RCA.

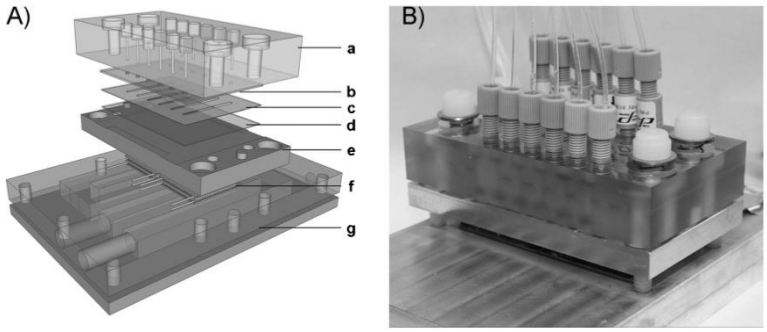

Figure 2.

Microfluidic device with temperature control. (A) Exploded view of the device with temperature control and integrated fluidics for automated heating, cooling, reagent loading, and washing; a: polycarbonate block with fluidic ports; b: glass slide with drilled holes; c: double-coated silicone adhesive tape; d: glass coverslip containing the DNA primer array; e: aluminum heating and cooling plate; f: thermoelectric modules; g: aluminum heat sink with channels for water cooling. Leak-free connections are made between the glass slide and the polycarbonate block using silicone O-rings (not shown). (B) Photograph of the assembled device.

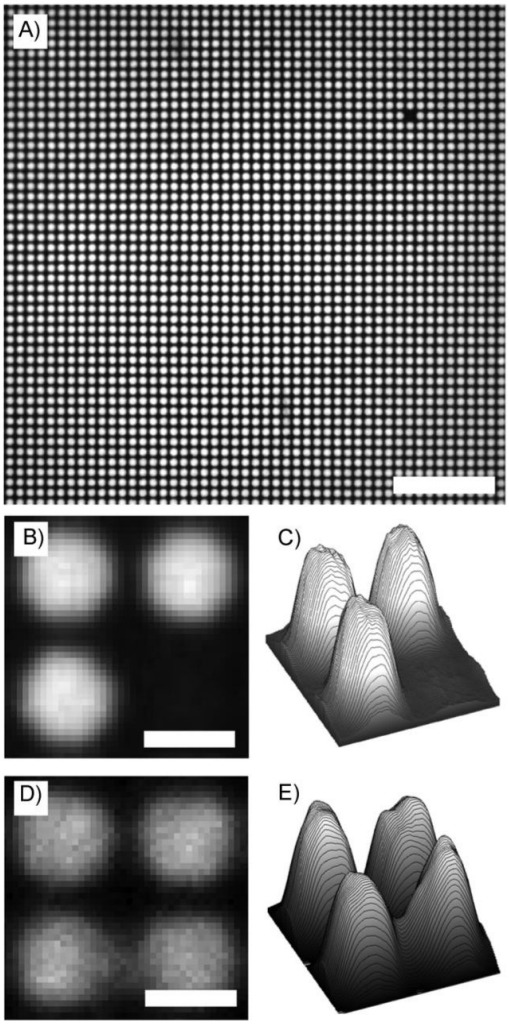

Figure 3.

High-density arrays of DNA polymer brushes. (A) Fluorescence image of a portion of an array of linear DNA polymers synthesized using RCA on an array of DNA primers; (B) Close-up view of a portion of the polymer array containing a missing polymer cluster. These dropouts occur when the posts in the photoresist are lost during development. The subsequent plasma treatment results in primer destruction in these unprotected regions; (C) Surface plot of the polymer clusters shown in (C); (D) Close-up view of a portion of the polymer array after a 30 min RCA reaction. With extended synthesis times, the linear polymers can become long enough to bridge adjacent clusters.; (E) Surface plot of the polymer clusters shown in (D). The scale bar is 40 μm in (A) and 3 μm in (B) and (D).

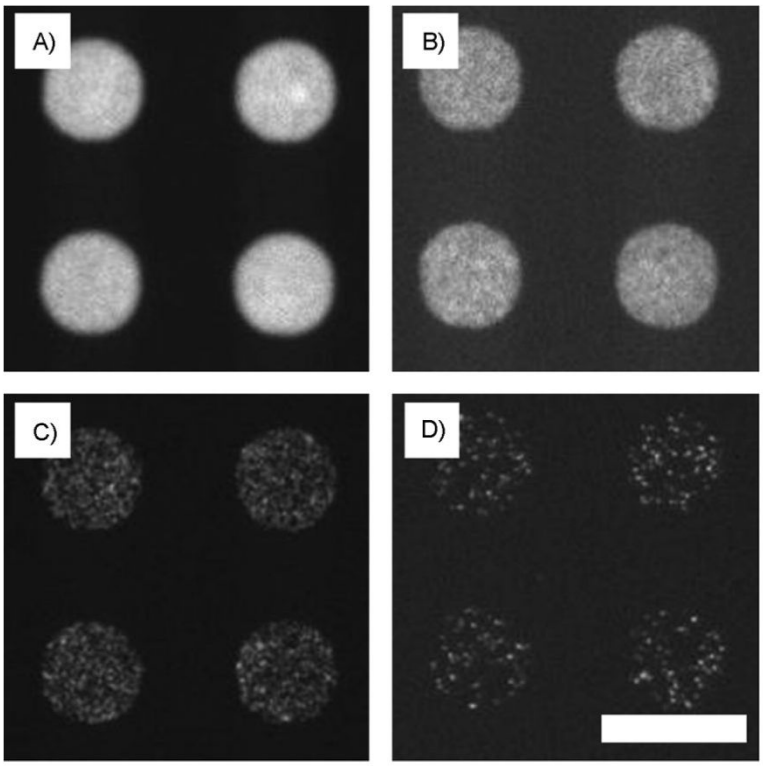

Figure 4.

Control of the density of DNA polymer brushes. Fluorescence images showing the effect of circular DNA template concentration on the density of the DNA polymer brushes. The circle concentrations were varied from 200 to 0.2×10^{-9} м: (A) 200×10^{-9} м, (B) 20×10^{-9} м, (C) 2×10^{-9} м, and (D) 0.2×10^{-9} м. The individual polymers can be resolved at the lower concentrations (C and D). These fluorescent micrographs were acquired with a 40× NA = 1.3 oil objective and an EMCCD camera with 8×8 μm^2 pixels. The scale bar is 15 μm.

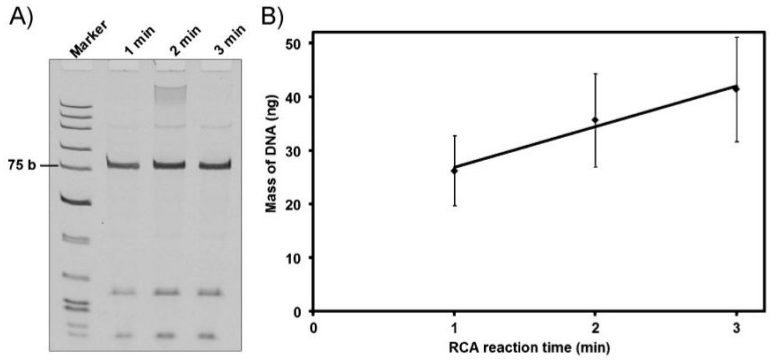

Figure 5.

Analysis of DNA polymer synthesis by enzymatic digestion and gel electrophoresis. (A) An image of a 20% polyacrylamide gel showing the result of an enzymatic digestion of the linear DNA polymers synthesized via solid-phase RCA. The primary bands in the right three lanes are 78-base fragments corresponding to the length of the circle used to synthesize the polymers. The higher bands correspond to fragments that are multiples of the 78-base fragment and are a result of incomplete digestion. The lower bands, which are 14 and 23 bases in length, are the digested products of the 37-base oligonucleotides that were hybridized to the polymers to introduce the restriction enzyme cutting sites. (B) A plot of the total amount of DNA synthesized per flow cell as a function of RCA reaction time. The growth rate is approximately linear in this range ($Y = 7.6X + 19.2$, $R^2 = 0.99$).

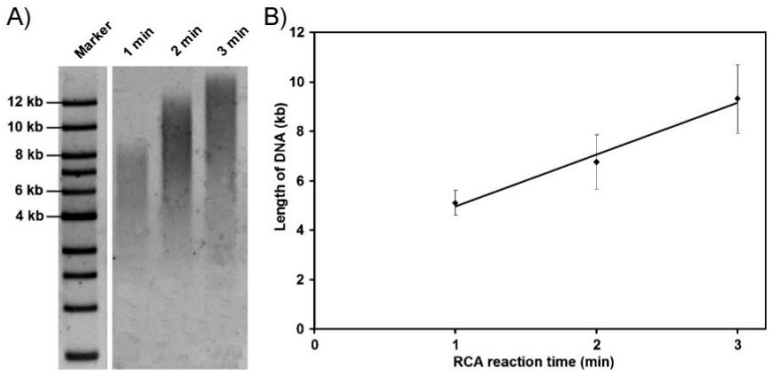

Figure 6.

Analysis of the DNA polymer length by enzymatic digestion and gel electrophoresis. (A) An image of a 0.5% agarose gel showing the average linear DNA polymer lengths for three different time points. The polymers were synthesized via solid-phase RCA, converted into a double-stranded form and then released from the substrate by cutting the molecules near the base with a restriction enzyme. (B) A plot of the average polymer length in kilobase pairs as a function of RCA reaction time. The polymer growth rate is approximately linear in this range ($Y = 2.1X + 2.9$, $R^2 = 0.98$).

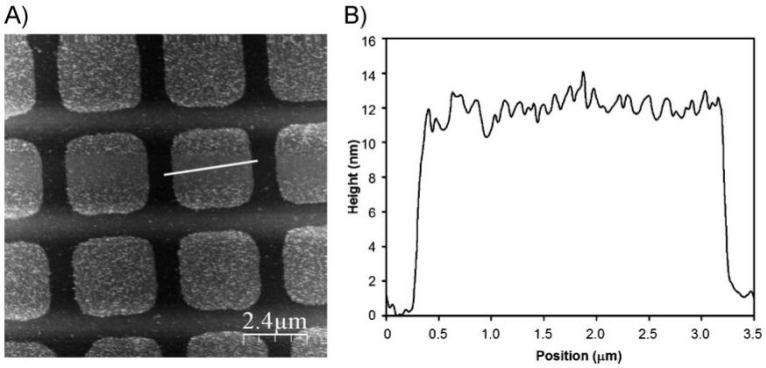

Figure 7.

Characterization of brush polymer arrays by AFM. (A) An AFM image of a 12 × 12 μm^2 portion of the polymer array. The array was produced by performing a 3-min RCA reaction after the hybridization of the 78-base circle at a concentration of 2×10^{-8} M to the primers on the surface. (B) Height profile of one feature of the brush array. The profile corresponds to the line shown in (A).